(p53 KD) in khES3 cells. Upregulation of p53 and phosphorylated p38 (p-p38), a downstream target of p53, were not observed in p53 KD cells 5 hr after Met deprivation (Figure 4G). p53 KD cells showed a partial rescue of the cell death induced by 48 hr Met deprivation (Figure 4H). Moreover, khES3 cells treated with a p38 inhibitor, SB239063 (SB), also showed a partial rescue of the cell death caused by Met deprivation (Figure 4I).

Our results indicate that activation of the p53-p38 signaling pathway is an early response at 5 hr, induced by Met deprivation. p38 activation partially accounts for the cell-cycle arrest, which leads to apoptosis of undifferentiated human ESCs/iPSCs upon prolonged Met deprivation.

Genes that were upregulated after Leu and Lys deprivation for 5 hr, but not after Met deprivation, were also identified (Figure S3A, Table S1C). Among these, DNA damage-inducible transcript 3 (*DDIT3*) increased significantly by real-time PCR analysis (Figure S3B). DDIT3, also known as C/EBP homologous protein (CHOP) and growth arrest and DNA damage-inducible gene 153 (GADD153), is an important component of the endoplasmic reticulum (ER) stress-mediated apoptosis pathway (Oyadomari and Mori, 2004). DDIT3 is induced by Leu depletion in human cell lines (Bruhat et al., 1997). These results, therefore, suggest that Leu and Lys deprivation induced apoptosis (Figure 1) *through a mechanism different from that of Met deprivation.*

Met Deprivation Reduced Histone and DNA Methylation, Decreased NANOG Expression, and Increased Overall Differentiation Potency

Our results showed that $[SAM]_i$ decreased rapidly within 5 hr of Met deprivation (Figure 2) and that treatment with SAM rescued Met deprivation-induced cell death (Figure 3A) and abolished upregulation of p53 (Figure 4E). SAM functions as a major methyl donor in methyl transfer reactions, such as methylation of histone H3 K4, K9, K27, and K36 and DNA methylation. A study in mouse ESCs demonstrated that SAM reduction decreased H3K4me3 (Shyh-Chang et al., 2013), but the effect of SAM reduction on epigenetic modifications of human ESCs/iPSCs is unknown. We thus examined the impact of Met deprivation on histone (Figures 5A and 5B) and DNA methylation (Figure 5C). After short-term (5 hr) Met deprivation in undifferentiated 201B7 cells, a rapid decrease in H3K4me3 was observed, which was reversed by the addition of SAM. Cycloleucine (100 mM) also decreased trimethylation of H3K4me3 levels (Figure 5A). Decreased H3K4me3 was also observed in khES3 cells (Figure 5B) and persisted under long-term (24 hr) Met deprivation (Figures 5A and 5B). Therefore, H3K4me3 demethylation occurred as a rapid response to decreased $[SAM]_i$ in human ESCs/iPSCs, similar to mouse ESCs. We also compared the extent of DNA methylation in undifferentiated 201B7 cells cultured for 5 hr in Met-deprived and complete media. A modest reduction in global DNA methylation was observed (Figure 5C), with 1,864 probes showing a decrease in Met-deprived cells greater than 15%, compared to those cultured in complete medium. Affected regions were not located at transcriptional start sites (TSSs) but were primarily in the vicinities of TSSs or gene body regions (Figure 5C). However, we could not identify specific genes regulated by Met deprivation (N.S., unpublished data). Taken together, our results indicate that Met deprivation results in a decrease in $[SAM]_i$, leading to a reduction in H3K4me3 and a global reduction in DNA methylation in human ESCs/iPSCs.

Decreased $[SAM]_i$ occurred 5 hr after Met deprivation and triggered p53-p38 activation (Figure 4). As p53 has been reported to induce differentiation of mouse ESCs by suppressing Nanog expression (Lin et al., 2005), we examined whether expression of pluripotent markers was affected. We found that NANOG expression decreased in undifferentiated 201B7 and khES3 cells after Met deprivation, while OCT3/4 expression was unaffected (Figures 5D and 5E). We next examined whether deprivation of other amino acids had an effect on *NANOG* and *OCT3/4* expression, and we found that Leu deprivation also triggered a decrease in *NANOG* expression, although to a level lower than that of Met deprivation. The decrease in *NANOG* expression was rescued by supplementation with Met or SAM in a concentration-dependent manner (Figures 5G and 5H).

We then tested whether a short period of Met deprivation increased the differentiation potency of human iPSCs (Figures 5I–5K). Pluripotent 201B7 cells were cultured in Met-deprived maintenance media for 10 hr and then subjected to differentiation into the definitive endoderm. The proportion and total number of $SOX17^+$ definitive endoderm cells increased in the Met-deprived group compared to the control group at differentiation day 4 (D4), indicating that Met deprivation potentiated differentiation into definitive endoderm (Figure 5I). However, gene expression profiling did not show marked induction of differentiation markers after Met deprivation at 5 or 24 hr (Figure S4A), suggesting that exposure to induction signals is required for triggering differentiation. Similar results were observed in khES1, khES3, and 253G1 iPSCs, indicating that potentiation of differentiation was commonly observed across different human ESC/iPSC lines (Figures S4B–S4D).

We then examined whether potentiation of differentiation occurs with differentiation into other germ layers. Undifferentiated 201B7 cells were cultured under Met-deprived conditions and then directed toward mesoderm differentiation. We observed a higher proportion of cells expressing the early mesoderm marker T protein (Figure 5J). Similarly, when deprived of Met and then directed to differentiate into ectodermal and neuronal lineages, expression levels of *PAX6* or *MAP2* increased compared to those cultured in complete media (Figure 5K).

Taken together, our results indicate that a short exposure to Met deprivation of undifferentiated human iPSCs decreased NANOG expression and increased the overall differentiation potency into the three germ layers.

(D) Relative khES3 (open bars) and 201B7 (black bars) cell numbers after culture for 48 hr in complete media with 0, 25, 50, or 100 mM cycloleucine (CL).
(E) Intracellular Met ($[Met]i$), SAM ($[SAM]i$), SAH ($[SAH]i$), and MTA ($[MTA]_i$) levels in undifferentiated khES3 cells 5 hr (open bars) or 24 hr (gray bars) after culture in *complete or 100 mM cycloleucine (CL100) media are shown. Data are normalized to DNA, and relative metabolite amounts are shown as a ratio of values at CL100* versus complete media.
(F) Relative cell numbers of cells treated for different time periods under control complete and Met-deprived conditions as shown in conditions a–c and d–f. Error bars represent SEM (n = 3). Significant differences compared to nonsupplemented cells (a and d) were determined by Student's t test; $^{**}p < 0.01$.

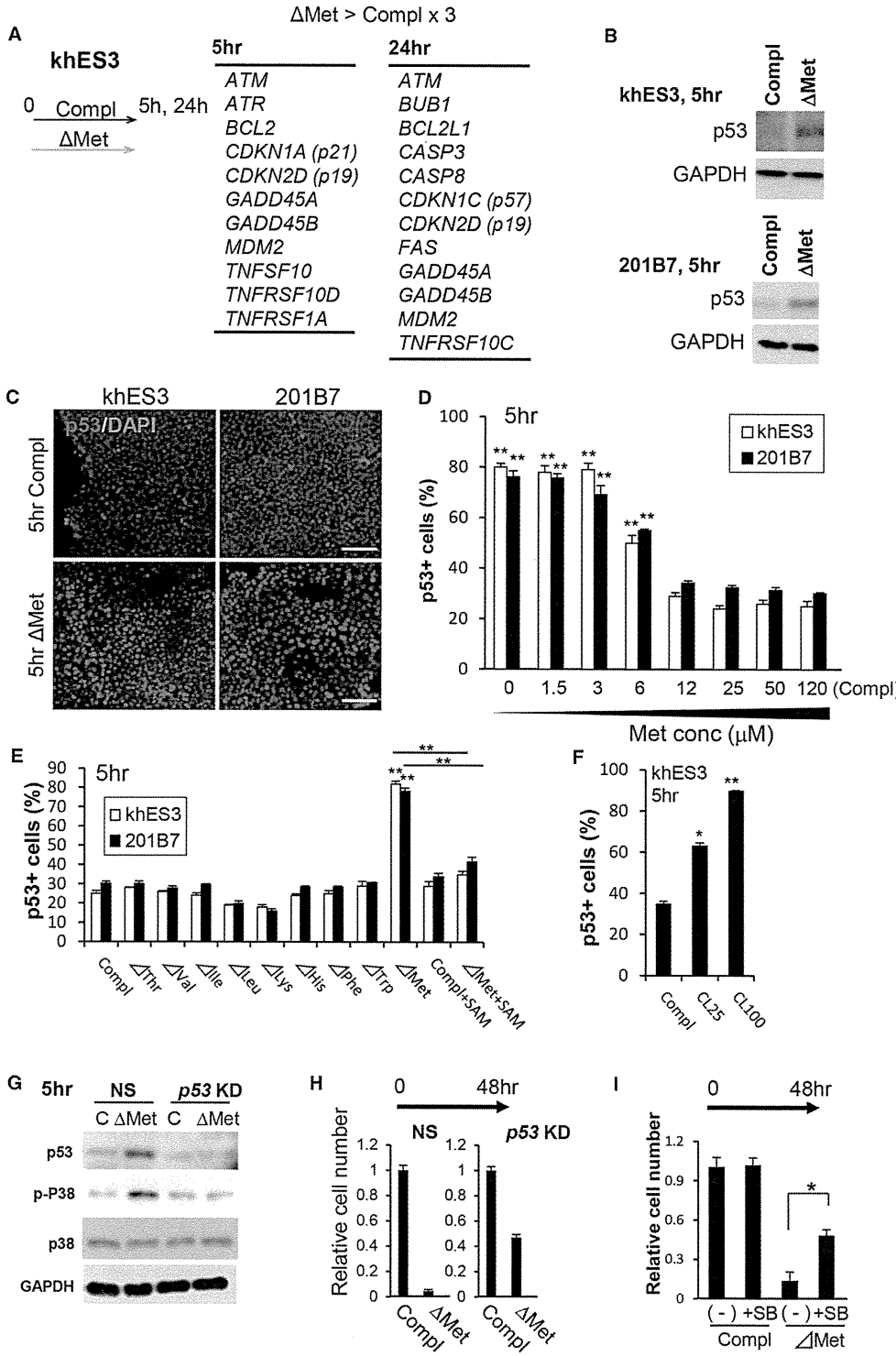

(legend on next page)

Undifferentiated Human ESCs Are in a High-Met Metabolic State Compared to Differentiated Cells

We previously established a procedure for inducing ESCs sequentially into the definitive endoderm as well as specific digestive organs, such as the pancreas, liver, and intestines (Ogaki et al., 2013; Shiraki et al., 2008a, 2008b, 2011). Marked differences exist in the differentiation potencies of human ESC/iPSC lines, which is an issue for efficient directed differentiation of human ESCs/iPSCs in vitro (Kajiwara et al., 2012; Osafune et al., 2008). We thus investigated differences in Met metabolism upon human ESC differentiation by focusing differentiation into the endoderm lineages.

We examined gene expression profiles, Met consumption, and Hcy excretion using undifferentiated khES3 cells, and the derived definitive endoderm cells differentiated under feeder-free conditions (Iwashita et al., 2013) (Figure 6A). Microarray analysis indicated that expression of essential Met and Cys metabolic enzymes, such as *DNMT*, was high in undifferentiated khES3 cells (Figure 6B). *MAT2A* expression was also elevated in undifferentiated khES3 cells, but downregulated in the definitive endoderm, whereas *MAT2B* levels were unchanged (Figure 6B).

The concentration of Met in the media rapidly decreased during maintenance culture, due to cellular uptake (Figure 6C). Total consumption of Met was significantly lower when cells adopted definitive endoderm differentiation compared to undifferentiated human ESCs. Furthermore, Hcy excretion from the endoderm was low and unaffected by Met deprivation (Figure 6D).

These results indicate that undifferentiated khES3 cells are in a high-flux Met metabolic state. In contrast, endoderm cells require a low amount of Met for cell growth and therefore are not affected by Met deprivation. This metabolic difference between undifferentiated cells and endoderm cells prompted us to test the effects of Met deprivation on eliminating remaining undifferentiated cells during differentiation.

Long-Term Met Deprivation Leads to Apoptosis, Specifically in Undifferentiated Cells, and Potentiates Endoderm and Hepatic Differentiation

Definitive endoderm differentiations of human ESC lines khES1 and khES3, and human iPSC lines 201B7 and 253G1 on day 10 (D10), are shown in Figure 7 (Shiraki et al., 2008a; Umeda et al., 2013). When khES3 or 253G1 cells were differentiated into definitive endoderm, OCT3/4 expression was rapidly downregulated. In contrast, in khES1 or 201B7 cells, a higher proportion of OCT3/4-expressing undifferentiated cells remained at D10 (Figure 7A). For hepatic differentiation, media was changed to hepatocyte differentiation media at D10 (Shiraki et al., 2008a; Umeda et al., 2013). The remaining undifferentiated cells were an obstacle for further differentiation, and expression of the early liver marker *AFP* and the hepatocyte marker albumin (*ALB*) in 201B7 cells was lower than that in khES3-derived differentiated cells (Figure 7B). Because Met deprivation triggered cell death in undifferentiated cells (Figure 1) without affecting Met metabolism in the definitive endoderm (Figure 6D), we deprived Met during mid-stage endoderm differentiation from day 8 (D8) to D10 in 201B7 cells. Met deprivation eliminated the undifferentiated OCT3/4 cells without affecting $SOX17^+$ cells (Figure 7C). We also tested khES1 cells, which are resistant to endoderm differentiation. Met deprivation also improved the differentiation efficiency of khES1 cells by eliminating undifferentiated cells (Figure 7D). Next, we analyzed the impact of Met deprivation on apoptosis. TUNEL-positive cells significantly increased with Met deprivation, which was observed in $OCT3/4^+$ cells, but not in $SOX17^+$ cells (Figure 7E). Quantitative measurements revealed that a high percentage of $OCT3/4^+$ cells (60%), but not $SOX17^+$ cells, rapidly became apoptotic upon Met deprivation (Figure 7F). As Met deprivation promoted cell death only in undifferentiated cells, we next examined its impact on hepatic differentiation. Met deprivation during D8–10 (Figures 7G–7I) potentiated the differentiation of 201B7 cells into the hepatic lineage, resulting in a remarkable increase in the proportion of AFP^+ cells and a reduction in $OCT3/4^+$ cells (Figure 7G). Met deprivation in 201B7 cells resulted in increased expression of *ALB* to a level even higher than that in primary hepatocytes (pHep) (Figure 7H), and secretion of ALB was higher than that in pHep as well (Figure 7I).

These data indicate that prolonged Met deprivation eliminates residual undifferentiated cells and leads to an increased overall differentiation efficiency in resistant cell lines, with respect to differentiation into endoderm and hepatic lineages.

DISCUSSION

In contrast to mouse ESCs, which are highly dependent on Thr metabolism, Tdh is nonfunctional in humans; moreover, we observed that undifferentiated pluripotent ESCs/iPSCs were in a high-Met metabolic state. We also found that SAM is required for the self-renewal of human ESCs/iPSCs and maintenance of an undifferentiated state. Short-term depletion of SAM triggered the following: (i) demethylation of H3K4me3, (ii) global DNA demethylation, (iii) p53 signaling activation, and (iv) decreased expression of the pluripotent marker NANOG. This then poised the cells in a potentiated state for differentiation into the three germ layers. In this state, MAT2A is upregulated, and the MTA

Figure 4. Met Deprivation Triggered Rapid Activation of p53-p38 Signaling in Pluripotent Human ESCs/iPSCs

(A) Gene expression profile analyses with undifferentiated khES3 cells showed that genes (signal intensity > 50) involved in the cell cycle or apoptosis are upregulated >3-fold in Met-deprived cells compared to cells cultured in control complete media.

(B and C) p53 expression in khES3 and 201B7 cells by western blot (B) or immunocytochemical analysis (C).

(D) The proportion of cells expressing p53 decreased with increasing Met concentration.

(E) Met deprivation, but not other amino acids, specifically increased $p53^+$ cells. SAM (100 μM) inhibited p53 accumulation in ΔMet conditions.

(F) Supplementation of 25 and 100 mM cycloleucine (CL25 and CL100) increased the number of $p53^+$ khES3 cells.

(G) p53 and phosphorylated p38 (p-p38) were upregulated 5 hr after Met deprivation in nonsilenced (NS) siRNA-treated ESCs, but neither p53 nor p-p38 increased in *p53* knockdown (KD) human ESCs.

(H) Decreased cell death in *p53* KD human ESCs after 48 hr Met deprivation.

(I) The p38 inhibitor, SB239063 (SB, 10 μM), rescued apoptosis. Error bars represent SEM (n = 3). Significant differences were determined by Student's t test; $^*p < 0.05$ and $^{**}p < 0.01$. Scale bar, 100 μm.

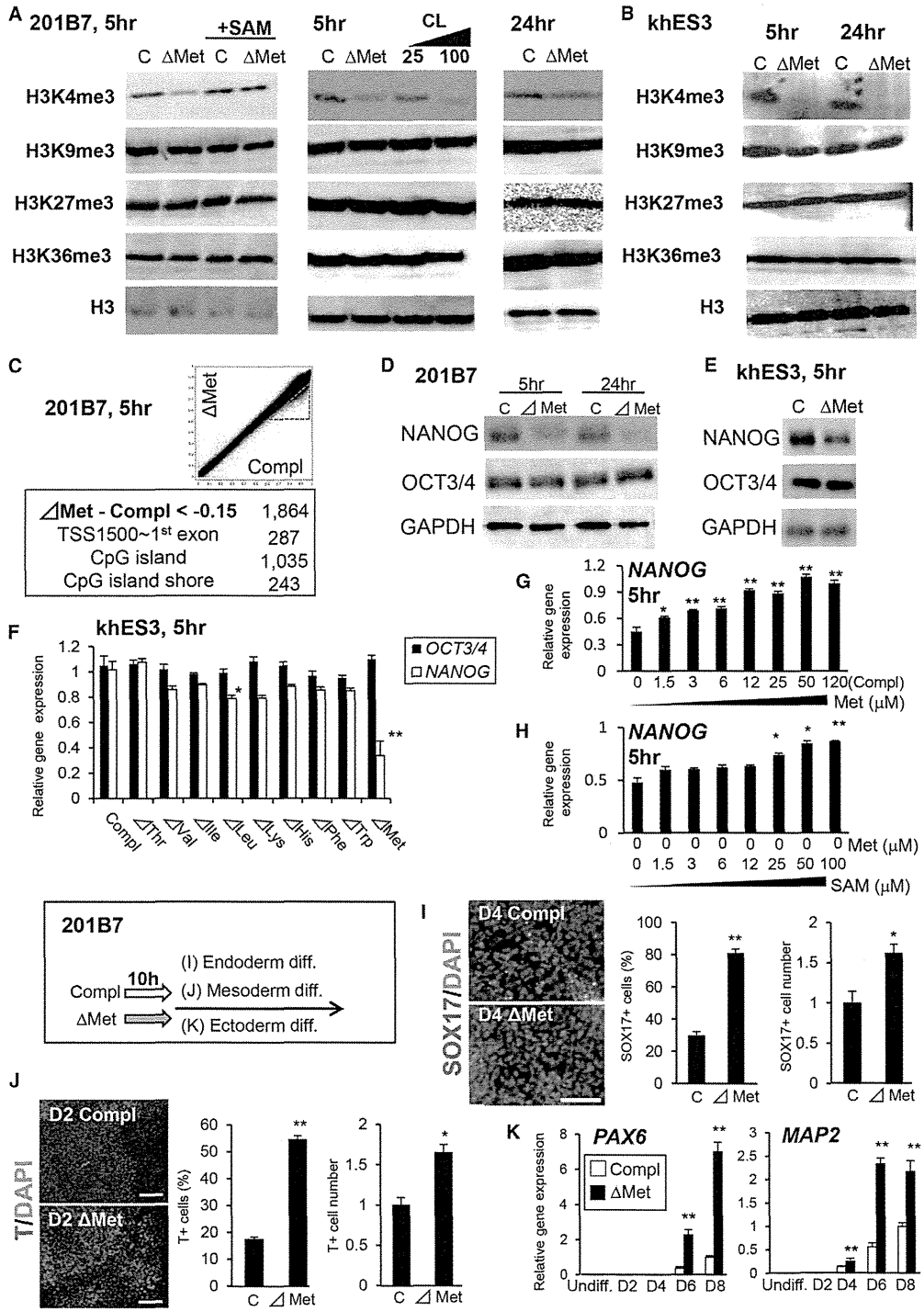

Figure 5. Short-Term Met Deprivation Triggers Histone and DNA Demethylation and Potentiates Differentiation into the Three Germ Layers

(A and B) Histone H3 methylation was examined in undifferentiated 201B7 (A) and khES3 (B) cells cultured in Met-deprived (ΔMet) or control media (C) for 5 or 24 hr. SAM supplementation (100 μM) in Met-deprived media (ΔMet+SAM) reversed demethylation of H3K4me3. Cycloleucine (100 mM) decreased H3K4me3 levels.

(legend continued on next page)

salvage pathway can replenish SAM. However, if Met depletion is prolonged and cells are not exposed to differentiation signals, the Met cycle eventually stops, and human ESCs/iPSCs undergo apoptosis.

Upon Met deprivation, cells halted excretion of Hcy and began to utilize SAM or MTA, resulting in reduced $[SAM]_i$ and $[MTA]_i$, a rapid response observed at 5 hr. *MAT2A* was upregulated to convert Met to SAM and restored the reduced $[SAM]_i$ 24 hr after Met deprivation. These events, such as salvage pathway activation and cessation of Hcy excretion, are stress responses of human ESCs/iPSCs revealed in this study. The pluripotent stem cells developed regulatory systems to maintain $[SAM]_i$ at constant levels. We also found that SAM supplementation rescued the apoptosis induced by Met deprivation, and supplementation of SAM, MTA, or Hcy rescued the impaired cell survival at a potency of SAM > MTA > Hcy. *MAT2A/MAT2B* knockdown or cycloleucine addition, but not *SMS* knockdown, phenocopied Met depletion and resulted in growth inhibition. Because cycloleucine specifically reduces $[SAM]_i$, but not $[Met]_i$, SAM, but not Met, is therefore essential for survival of undifferentiated human ESCs/iPSCs.

SAM is a major methyl donor during methyl transfer reactions, including histone or DNA methylation. Histone methylation contributes to chromatin remodeling as well as transcriptional activity (Berger, 2007). SAM functions as a sensor for Met metabolism, with a rapid decrease in $[SAM]_i$ inducing H3K4me3 and DNA demethylation, as well as decreased NANOG expression and p53-p38 pathway activation. Met deprivation rapidly poised human ESCs/iPSCs for differentiation. However, prolonged exposure to Met deprivation for 24 hr or more in the absence of appropriate differentiation signals caused the cells to undergo an irreversible change, such as prolonged G0/G1 arrest and decreased self-renewal, thus triggering apoptosis. When deprival of Met was performed during mid-stage differentiation, residual undifferentiated cells were eliminated, and overall differentiation efficiency was increased. Therefore, this knowledge is useful and applicable to eliminate variability in differentiation efficiency among cell lines and promote differentiation into specific lineages. Human iPSCs are reportedly dependent on oleate; an inhibitor of oleate synthesis shows cytotoxicity and may selectively eliminate human iPSCs (Ben-David et al., 2013). Cardiomyocytes and noncardiomyocytes from mouse and human ESCs/iPSCs differ markedly in glucose and lactate metabolism; thus, cardiomyocytes can be obtained at a high purity during large-scale purification by culture in glucose-free media (Tohyama et al., 2013). However, culture in glucose-free media did not potentiate differentiation, which differs from our present results regarding short-term Met deprivation.

While methylation of H3K4 is generally associated with activation of transcription, H3K9 and H3K27 are repressive epigenetic markers. In ESCs, simultaneous methylation of H3K4 and H3K27 is associated with the undifferentiated state, where a gene may be poised to be either fully activated or repressed (Bernstein et al., 2006). Here, decreased trimethylation of H3K4 (H3K4me3) resulting from Met deprivation suggests that Met metabolism might function in the regulation of self-renewal of pluripotent stem cells through epigenetic marking at H3K4me3 (Ang et al., 2011). Previously, mouse ESCs were reported to be in a high-flux state requiring Thr to maintain cell-cycle progression (Wang et al., 2009). In mouse ESCs, rapid conversion of Thr to Gly by Tdh is suggested to provide 5-methyltetrahydrofolate (5mTHF) needed for recycling SAH to SAM; thus, Thr deprivation caused a reduction in SAM, which then triggered demethylation of H3K4me3 and H3K4me2 (Shyh-Chang et al., 2013). In humans, the *TDH* gene is an expressed pseudogene (Edgar, 2002). Human ESCs/iPSCs directly generate SAM from Met. Therefore, mouse and human ESCs/iPSCs utilize similarly the Met pathway for maintaining their pluripotent state in principal. Met metabolism directly regulates SAM levels, and SAM reduction triggered demethylation of H3K4me3 (but not H3K9me3, H3K27me3, or H3K36me3) specifically, the mechanism of which remains unknown.

Evidence suggests that self-renewal and pluripotency are closely linked to cell-cycle regulation in pluripotent stem cells and that NANOG plays a role in the G1-to-S transition through direct binding of *CDK6* and *CDC25A* (Zhang et al., 2009). The high self-renewal rate is considered essential for maintaining ESC identity, and cell-cycle arrest is sufficient to drive human ESCs toward irreversible differentiation (Ruiz et al., 2011). Deletion of p53 in mouse cells or silencing of p53 in human somatic cells increases the reprogramming efficiency (Kawamura et al., 2009). p53 induces differentiation by directly suppressing NANOG expression in mouse ESCs (Lin et al., 2005). Our results showed that Met deprivation triggered decreased expression of NANOG, but not OCT3/4. NANOG is a member of the core transcription circuit required for ESCs to maintain pluripotency. While NANOG is actively downregulated during differentiation, OCT3/4 is downregulated when the later lineage choice occurs (Iovino and Cavalli, 2011). Our present results suggest that the Met metabolism is responsible for regulation of cell-cycle progression and maintenance of pluripotency of human ESCs/iPSCs versus differentiation or apoptosis through the p53-p38 signaling pathway. Activation of p53 signaling was observed specifically under conditions of Met deprivation but was not seen upon deprivation of other amino acids, and p53-p38 accumulation was halted by the addition of SAM.

(C) DNA methylation profiles in undifferentiated 201B7 cells cultured in complete medium (x axis) and Met-deprived medium (y axis) for 5 hr. The number of probes with greater than 15% reduction in DNA methylation under Met deprivation are shown.
(D and E) Short-term Met deprivation (5 hr) downregulated NANOG expression in 201B7 (D) and khES3 (E) cells.
(F) Real-time PCR analysis of *NANOG* and *OCT3/4* in khES3 cells in complete or amino acid-deprived media for 5 hr.
(G and H) *NANOG* expression increased with increasing Met (G) or SAM (H) concentration in the media.
(I–K) Human iPSCs cultured in Met-deprived conditions showed an elevated differentiation into the definitive endoderm (I), mesoderm (J), and ectoderm (K), as shown by expression of the endoderm marker SOX17 (I), early mesoderm marker T (J), *PAX*, or *MAP2* (K) by immunohistochemical (I and J) or real-time PCR (K) analyses. Cells were pretreated with complete medium (I and J, left bars; K, open bars) or Met-deprived media (I and J, right bars; K, black bars) before differentiation. Error bars represent SEM (n = 3). Student's t test; $^*p < 0.05$ and $^{**}p < 0.01$. Scale bar, 100 μm.

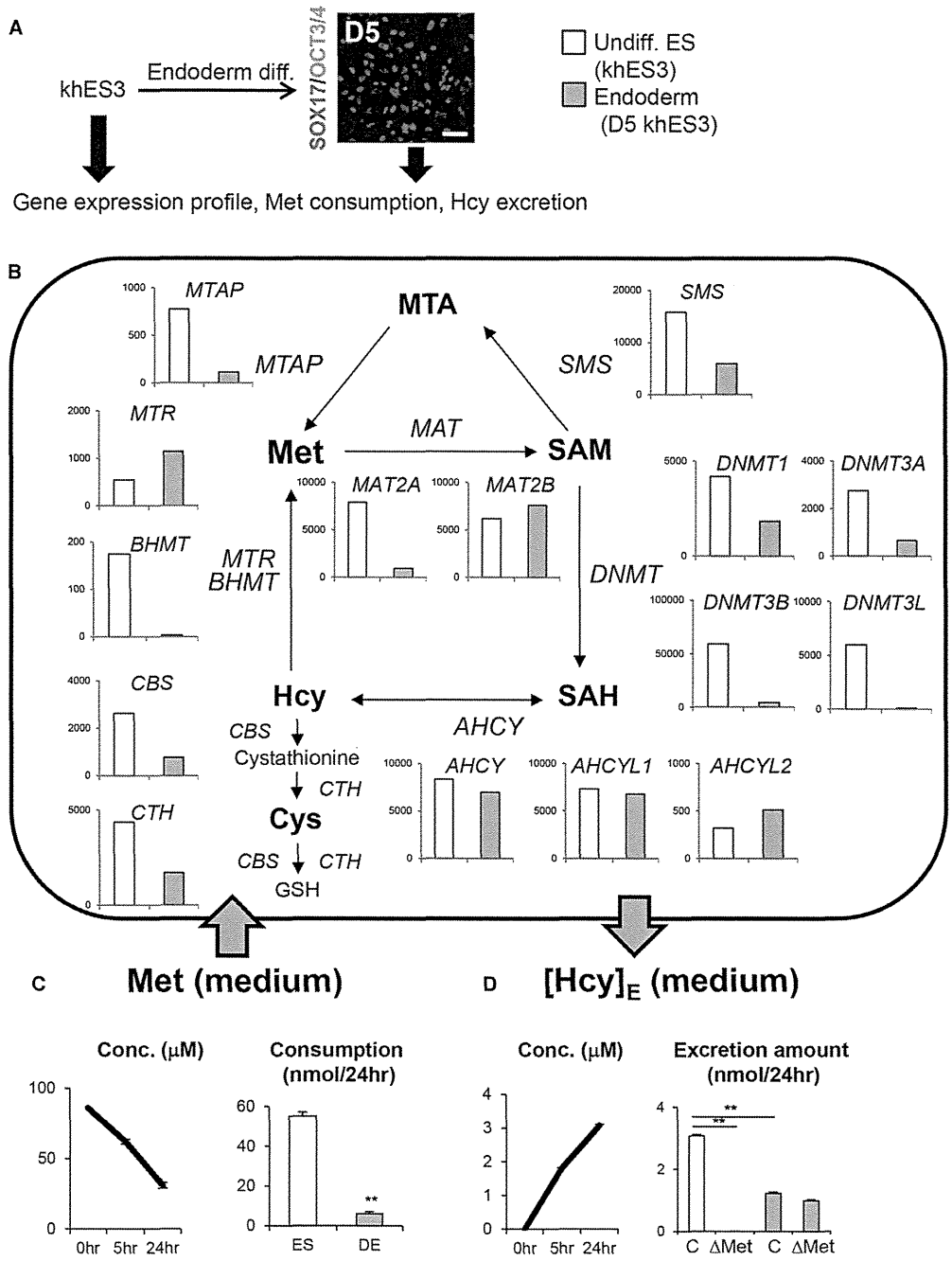

Figure 6. Undifferentiated Human ESCs Are in a High-Met Metabolic State Compared with Definitive Endoderm Cells

(A) Schematic drawings of the experimental design to determine differences in Met metabolism between undifferentiated ESCs and definitive endoderm cells. Endoderm cells differentiated for 5 days expressed SOX17, but not OCT3/4.

(B) Signal intensity of Met cycle-related genes in undifferentiated (undiff) and differentiated khES3 cells on differentiation day 5 (D5) toward the definitive endoderm analyzed by microarray.

(legend continued on next page)

SAM has been reported to act as a stress sensor in malignant cells (Lin et al., 2014). P53 is also known to trigger various stress responses (Kruse and Gu, 2009). We found that 5 hr Met deprivation in khES3 cells triggered a 27-fold increase in the expression of *EGR1*, a transcription factor that upregulates *p53* (Baron et al., 2006), or a 33-fold increase in *DHRS2*, a gene that inhibits Mdm2 and stabilizes p53 protein (Deisenroth et al., 2010). Therefore, Egr1 and DHRS2 are candidate molecules that mediate upregulation of p53 triggered by SAM limitation. However, the exact molecular mechanism linking SAM and p53 still awaits future investigations.

Taken together, our data indicate that Met deprivation results in a rapid decrease in $[SAM]_i$, triggering activation of p53-p38 signaling, reducing NANOG expression, and poising human iPSC/ESCs for differentiation. The cells endured short-term Met deprivation by replenishing the $[Met]_i$ pool with the salvage Met pathway, which was then metabolized to replenish SAM. However, during prolonged Met deprivation, the continued absence of Met metabolism led to cell-cycle arrest and apoptosis. These results are consistent with the data from previous studies indicating that p53 is a barrier to reprogramming and that decreasing p53 protein levels increases the efficiency of reprogramming (Banito et al., 2009; Kawamura et al., 2009). In conclusion, we demonstrated the importance of SAM in Met metabolism in regulating p53 signaling and its relationship with pluripotency, cell survival, and differentiation of human ESCs/iPSCs. Our findings can be utilized to eliminate undifferentiated pluripotent cells in culture and may be useful for future applications in regenerative medicine.

EXPERIMENTAL PROCEDURES

Cell Culture and Reagents

Human ESCs were approved by Kumamoto University's Institutional Review Board, following the hESC guidelines of the Japanese government. Undifferentiated human ESCs (khES1, khES3) (Suemori et al., 2006) and iPSCs (201B7, 253G1) (Takahashi et al., 2007) were maintained as described (Shiraki et al., 2008a). For feeder-free culture, ESCs/iPSCs were cultured on matrigel-coated dish with feeder-free culture media ReproFF (ReproCELL). For Met deprivation with undifferentiated cells, cells were cultured with human ESC/iPSC maintenance medium CSTI-7 (Cell Science & Technology Institute; CSTI) (Furue et al., 2008) or Met-deprived CSTI-7 medium. Met, Hcy, Cys, SAM, MTA, cycloleucine, and SAH were purchased from Sigma-Aldrich. SB239063 was purchased from Calbiochem. Methods of endoderm, mesoderm, or ectoderm differentiation, and gene knockdown examination, are described in Supplemental Experimental Procedures.

Real-Time PCR, Immunocytochemistry, and Western Blot Analysis

Real-time PCR, immunocytochemistry, and western blot were performed as previously described (Shiraki et al., 2011). Primer sequences and antibody information are shown in Tables S2 and S3, respectively. In immunocytochemical analysis, positive cells versus total cells (DAPI-positive cells) were quantified using ImageXpress Micro cellular imaging system (Molecular Devices).

Measurement of Met, SAM, SAH, MTA, and Hcy

Measurement of methionine, SAM, SAH, MTA, and Hcy was performed using ultra-high-performance liquid chromatography equipped with tandem mass spectrometry, TQD (UPLC-MS/MS; Waters) based on a previous report (Jiang et al., 2009). Separation was achieved using an ACQUITY UPLC BEH C18 column. Briefly, cells were lysed using three cycles of freeze/thaw in 50% methanol. Samples were deproteinized using 33% acetonitrile and evaporated completely. Pellets were dissolved in 10 mM HCl, followed by filtration using 0.22 μm polyvinylidene fluoride (PVDF) filter (Millipore) and diluted with equal volumes of either 50 mM Tris-HCl (pH 8.8) with 100 μm dithiothreitol (DTT) for Met, SAM, and SAH or 20 mM formic acid for MTA. For Hcy analysis in the media, cultured media were collected and incubated for 10 min at 37°C with 10 mM DTT to obtain total Hcy secreted from the cells. Media were deproteinized using 50% acetonitrile, followed by filtration, and then diluted with equal volumes of 50 mM Tris-HCl (pH 8.8). Each sample was injected, and concentrations were calculated based on the standard curve obtained from serial dilution of standard solution for each metabolite.

Microarray Analysis

Affymetrix H133 Plus 2.0 series probe array (GeneChip) was used. Expression analysis was performed using the Subio Platform (Subio).

Cell-Cycle Analysis

Fixed cells were stained with DAPI and anti-phospho Histone H3 Ser10 (pH3; Millipore). Images were acquired on the ImageXpress Micro and analyzed using the Cell Cycle Application Module (Molecular Devices).

Apoptosis Assay

Apoptosis was detected by the TUNEL method using an In Situ Cell Death Detection Kit (Roche).

Measurement of Cell Proliferation

Cell proliferation was measured by the incorporation of EdU into genomic DNA during the S phase of the cell cycle, using Click-iT EdU Kit (Invitrogen).

Functional Assays for Hepatocytes

Albumin secretion assay was performed as described (Shiraki et al., 2011). Cryopreserved human hepatocytes (Invitrogen) cultured 24 hr on collagen I coated plates with hepatocyte maintenance medium (Invitrogen) were used as positive controls.

Methylation Profiling

Methylation profiling analysis was performed as described (Nagae et al., 2011). Methylation status was analyzed using the Human Methylation 450 BeadChip (Illumina).

Statistical Analysis

Error bars represent SEM. The significance of differences between two groups was analyzed by Student's t test and presented as $^*p < 0.05$ or $^{**}p < 0.01$.

ACCESSION NUMBERS

Microarray data have been deposited under Gene Expression Omnibus (GEO) accession number GSE55285.

SUPPLEMENTAL INFORMATION

Supplemental Information includes Supplemental Experimental Procedures, four figures, and three tables and can be found with this article online at http://dx.doi.org/10.1016/j.cmet.2014.03.017.

AUTHOR CONTRIBUTIONS

N.S. and Y.S. designed the experiments and performed cellular and biochemical analyses to check the effect of Met in differentiation stages. N.S.

(C) Time-dependent changes in Met concentration 5 or 24 hr after culture in complete media (left). Met consumption at 24 hr in undifferentiated or endoderm cells (*right*).

(D) Time-dependent excretion of Hcy 5 or 24 hr after culture in complete media. Excreted Hcy ($[Hcy]_E$) at 24 hr in undifferentiated or endoderm cells grown in complete or Met-deprived media. Error bars represent SEM (n = 3). Student's t test; $^{**}p < 0.01$. Scale bar, 100 μm. Open bars, undifferentiated cells; gray bars, definitive endoderm.

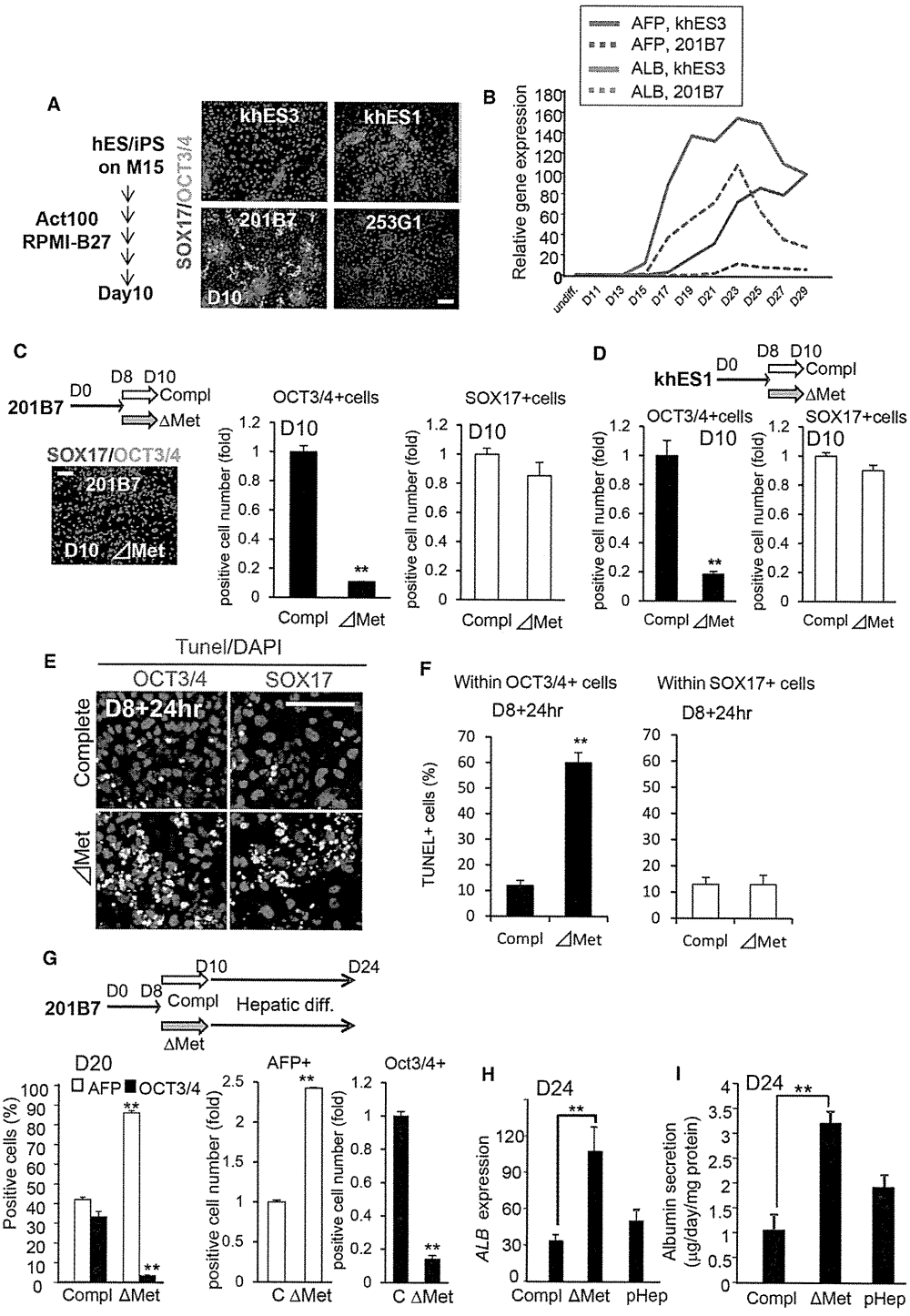

(legend on next page)

performed cellular and biochemical analyses to check the effect of Met in the undifferentiation stage and wrote the paper. T.T. handled the collection and assembly of data. F.O. and M.M. performed the measurement of Met-cycle metabolites. G.N. and H.A. performed the analysis of global DNA methylation. K.K. provided technical advice and helpful discussions. F.E. conceived the study and provided technical advice and financial support. S.K. conceived the study and design, wrote the paper, interpreted results, provided financial support, and finalized the manuscript.

ACKNOWLEDGMENTS

We thank Drs. Norio Nakatsuji and Hirofumi Suemori (Kyoto University) for providing khES1 and khES3 cells and Dr. Shinya Yamanaka (Kyoto University) for providing 201B7 and 253G1 iPSC lines. We thank Ms. Nigar Sultana, Akiko Harada, and the members of the Gene Technology Center at Kumamoto University for their technical assistance. This work was supported by a grant from the National Institute of Biomedical Innovation (to N.S.); the NEXT Program (to S.K.) by the Japanese Society for the Promotion of Science (JSPS); and a grant from the Project for Realization of Regenerative Medicine from the Ministry of Education, Culture, Sports, Science and Technology (MEXT) Japan (to S.K. and F.E.). This work was also supported in part by the Program for Leading Graduate Schools "HIGO (Health life science; Interdisciplinary and Glocal Oriented) Program" (to S.K.), from MEXT. S.K. is a member of the Program for Leading Graduate Schools "HIGO."

Received: September 22, 2013
Revised: January 9, 2014
Accepted: March 11, 2014
Published: April 17, 2014

REFERENCES

Alexander, P.B., Wang, J., and McKnight, S.L. (2011). Targeted killing of a *mammalian cell based upon its specialized metabolic state. Proc.* Natl. Acad. Sci. USA *108*, 15828–15833.

Ang, Y.S., Tsai, S.Y., Lee, D.F., Monk, J., Su, J., Ratnakumar, K., Ding, J., Ge, Y., Darr, H., Chang, B., et al. (2011). Wdr5 mediates self-renewal and reprogramming via the embryonic stem cell core transcriptional network. Cell *145*, 183–197.

Armstrong, L., Tilgner, K., Saretzki, G., Atkinson, S.P., Stojkovic, M., Moreno, R., Przyborski, S., and Lako, M. (2010). Human induced pluripotent stem cell lines show stress defense mechanisms and mitochondrial regulation similar to those of human embryonic stem cells. Stem Cells *28*, 661–673.

Banito, A., Rashid, S.T., Acosta, J.C., Li, S., Pereira, C.F., Geti, I., Pinho, S., Silva, J.C., Azuara, V., Walsh, M., et al. (2009). Senescence impairs successful reprogramming to pluripotent stem cells. Genes Dev. *23*, 2134–2139.

Baron, V., Adamson, E.D., Calogero, A., Ragona, G., and Mercola, D. (2006). The transcription factor Egr1 is a direct regulator of multiple tumor suppressors including TGFbeta1, PTEN, p53, and fibronectin. Cancer Gene Ther. *13*, 115–124.

Ben-David, U., Gan, Q.F., Golan-Lev, T., Arora, P., Yanuka, O., Oren, Y.S., Leikin-Frenkel, A., Graf, M., Garippa, R., Boehringer, M., et al. (2013). Selective elimination of human pluripotent stem cells by an oleate synthesis inhibitor discovered in a high-throughput screen. Cell Stem Cell *12*, 167–179.

Berger, S.L. (2007). The complex language of chromatin regulation during transcription. Nature *447*, 407–412.

Bernstein, B.E., Mikkelsen, T.S., Xie, X., Kamal, M., Huebert, D.J., Cuff, J., Fry, B., Meissner, A., Wernig, M., Plath, K., et al. (2006). A bivalent chromatin structure marks key developmental genes in embryonic stem cells. Cell *125*, 315–326.

Boheler, K.R. (2009). Stem cell pluripotency: a cellular trait that depends on transcription factors, chromatin state and a checkpoint deficient cell cycle. J. Cell. Physiol. *221*, 10–17.

Bruhat, A., Jousse, C., Wang, X.Z., Ron, D., Ferrara, M., and Fafournoux, P. (1997). Amino acid limitation induces expression of CHOP, a CCAAT/enhancer binding protein-related gene, at both transcriptional and post-transcriptional levels. J. Biol. Chem. *272*, 17588–17593.

Deisenroth, C., Thorner, A.R., Enomoto, T., Perou, C.M., and Zhang, Y. (2010). Mitochondrial Hep27 is a c-Myb target gene that inhibits Mdm2 and stabilizes p53. Mol. Cell. Biol. *30*, 3981–3993.

Edgar, A.J. (2002). The human L-threonine 3-dehydrogenase gene is an expressed pseudogene. BMC Genet. *3*, 18.

Facucho-Oliveira, J.M., and St John, J.C. (2009). The relationship between pluripotency and mitochondrial DNA proliferation during early embryo development and embryonic stem cell differentiation. Stem Cell Rev. *5*, 140–158.

Finkelstein, J.D. (1990). Methionine metabolism in mammals. J. Nutr. Biochem. *1*, 228–237.

Folmes, C.D., Nelson, T.J., Martinez-Fernandez, A., Arrell, D.K., Lindor, J.Z., Dzeja, P.P., Ikeda, Y., Perez-Terzic, C., and Terzic, A. (2011). Somatic oxidative bioenergetics transitions into pluripotency-dependent glycolysis to facilitate nuclear reprogramming. Cell Metab. *14*, 264–271.

Furue, M.K., Na, J., Jackson, J.P., Okamoto, T., Jones, M., Baker, D., Hata, R., Moore, H.D., Sato, J.D., and Andrews, P.W. (2008). Heparin promotes the growth of human embryonic stem cells in a defined serum-free medium. Proc. Natl. Acad. Sci. USA *105*, 13409–13414.

Goll, M.G., and Bestor, T.H. (2005). Eukaryotic cytosine methyltransferases. Annu. Rev. Biochem. *74*, 481–514.

Halim, A.B., LeGros, L., Geller, A., and Kotb, M. (1999). Expression and functional interaction of the catalytic and regulatory subunits of human methionine adenosyltransferase in mammalian cells. J. Biol. Chem. *274*, 29720–29725.

Iovino, N., and Cavalli, G. (2011). Rolling ES cells down the Waddington landscape with Oct4 and Sox2. Cell *145*, 815–817.

Iwashita, H., Shiraki, N., Sakano, D., Ikegami, T., Shiga, M., Kume, K., and Kume, S. (2013). Secreted cerberus1 as a marker for quantification of definitive endoderm differentiation of the pluripotent stem cells. PLoS ONE *8*, e64291.

Jiang, Z., Liang, Q., Luo, G., Hu, P., Li, P., and Wang, Y. (2009). HPLC-electrospray tandem mass spectrometry for simultaneous quantitation of eight plasma aminothiols: application to studies of diabetic nephropathy. Talanta *77*, 1279–1284.

Kajiwara, M., Aoi, T., Okita, K., Takahashi, R., Inoue, H., Takayama, N., Endo, H., Eto, K., Toguchida, J., Uemoto, S., and Yamanaka, S. (2012). Donor-dependent variations in hepatic differentiation from human-induced pluripotent stem cells. Proc. Natl. Acad. Sci. USA *109*, 12538–12543.

Figure 7. Met Deprivation Potentiates Hepatic Differentiation

(A) khES1, khES3, 201B7, and 253G1 cells were subjected to endodermal differentiation using M15 feeder cells (Shiraki et al., 2008a; Umeda et al., 2013). SOX17 (red) and OCT3/4 (green) expression was detected by immunocytochemistry.

(B) *AFP* (red) or *ALB* (blue) mRNA expression was detected by real-time PCR. Expression in khES3 (solid lines) or 201B7 cells (broken lines).

(C and D) Impact of Met deprivation on the remaining $OCT3/4^+$ undifferentiated cells (black bars) or $SOX17^+$ definitive endoderm cells (open bars) derived from 201B7 cells (C) or khES1 cells (D).

(E) Fluorescent image of TUNEL staining.

(F) Quantitative analysis of TUNEL-positive cells.

(G–I) The impact of Met deprivation on hepatic differentiation. (G) Proportions and number of AFP^+ cells (open bars) or $OCT3/4^+$ cells (black bars) in complete or Met-deprived media. (H and I) Upon Met deprivation, increased *ALB* expression (H) and ALB secretion on D24 (I) were observed. pHep, primary human hepatocytes. Error bars represent SEM (n = 3). Significant differences were determined by Student's t test; $^{**}p < 0.01$. Scale bar, 100 μm.

Kawamura, T., Suzuki, J., Wang, Y.V., Menendez, S., Morera, L.B., Raya, A., Wahl, G.M., and Izpisúa Belmonte, J.C. (2009). Linking the p53 tumour suppressor pathway to somatic cell reprogramming. Nature *460*, 1140–1144.

Kruse, J.P., and Gu, W. (2009). Modes of p53 regulation. Cell *137*, 609–622.

Lin, T., Chao, C., Saito, S., Mazur, S.J., Murphy, M.E., Appella, E., and Xu, Y. (2005). p53 induces differentiation of mouse embryonic stem cells by suppressing Nanog expression. Nat. Cell Biol. *7*, 165–171.

Lin, D.W., Chung, B.P., and Kaiser, P. (2014). S-adenosylmethionine limitation induces p38 mitogen-activated protein kinase and triggers cell cycle arrest in G1. J. Cell Sci. *127*, 50–59.

Lu, S.C., and Mato, J.M. (2008). S-Adenosylmethionine in cell growth, apoptosis and liver cancer. J. Gastroenterol. Hepatol. *23* (*Suppl 1*), S73–S77.

Nagae, G., Isagawa, T., Shiraki, N., Fujita, T., Yamamoto, S., Tsutsumi, S., Nonaka, A., Yoshiba, S., Matsusaka, K., Midorikawa, Y., et al. (2011). Tissue-specific demethylation in CpG-poor promoters during cellular differentiation. Hum. Mol. Genet. *20*, 2710–2721.

Ogaki, S., Shiraki, N., Kume, K., and Kume, S. (2013). Wnt and Notch signals guide embryonic stem cell differentiation into the intestinal lineages. Stem Cells *31*, 1086–1096.

Osafune, K., Caron, L., Borowiak, M., Martinez, R.J., Fitz-Gerald, C.S., Sato, Y., Cowan, C.A., Chien, K.R., and Melton, D.A. (2008). Marked differences in differentiation propensity among human embryonic stem cell lines. Nat. Biotechnol. *26*, 313–315.

Oyadomari, S., and Mori, M. (2004). Roles of CHOP/GADD153 in endoplasmic reticulum stress. Cell Death Differ. *11*, 381–389.

Ruiz, S., Panopoulos, A.D., Herrerías, A., Bissig, K.D., Lutz, M., Berggren, W.T., Verma, I.M., and Izpisua Belmonte, J.C. (2011). A high proliferation rate is required for cell reprogramming and maintenance of human embryonic stem cell identity. Curr. Biol. *21*, 45–52.

Shi, Y. (2007). Histone lysine demethylases: emerging roles in development, physiology and disease. Nat. Rev. Genet. *8*, 829–833.

Shiraki, N., Umeda, K., Sakashita, N., Takeya, M., Kume, K., and Kume, S. (2008a). Differentiation of mouse and human embryonic stem cells into hepatic lineages. Genes Cells *13*, 731–746.

Shiraki, N., Yoshida, T., Araki, K., Umezawa, A., Higuchi, Y., Goto, H., Kume, K., and Kume, S. (2008b). Guided differentiation of embryonic stem cells into Pdx1-expressing regional-specific definitive endoderm. Stem Cells *26*, 874–885.

Shiraki, N., Yamazoe, T., Qin, Z., Ohgomori, K., Mochitate, K., Kume, K., and Kume, S. (2011). Efficient differentiation of embryonic stem cells into hepatic cells in vitro using a feeder-free basement membrane substratum. PLoS ONE *6*, e24228.

Shyh-Chang, N., Locasale, J.W., Lyssiotis, C.A., Zheng, Y., Teo, R.Y., Ratanasirintrawoot, S., Zhang, J., Onder, T., Unternaehrer, J.J., Zhu, H., et al. (2013). Influence of threonine metabolism on S-adenosylmethionine and histone methylation. Science *339*, 222–226.

Suemori, H., Yasuchika, K., Hasegawa, K., Fujioka, T., Tsuneyoshi, N., and Nakatsuji, N. (2006). Efficient establishment of human embryonic stem cell lines and long-term maintenance with stable karyotype by enzymatic bulk passage. Biochem. Biophys. Res. Commun. *345*, 926–932.

Sufrin, J.R., Coulter, A.W., and Talalay, P. (1979). Structural and conformational analogues of L-methionine as inhibitors of the enzymatic synthesis of S-adenosyl-L-methionine. IV. Further mono-, bi- and tricyclic amino acids. Mol. Pharmacol. *15*, 661–677.

Takahashi, K., Tanabe, K., Ohnuki, M., Narita, M., Ichisaka, T., Tomoda, K., and Yamanaka, S. (2007). Induction of pluripotent stem cells from adult human fibroblasts by defined factors. Cell *131*, 861–872.

Takubo, K., Nagamatsu, G., Kobayashi, C.I., Nakamura-Ishizu, A., Kobayashi, H., Ikeda, E., Goda, N., Rahimi, Y., Johnson, R.S., Soga, T., et al. (2013). Regulation of glycolysis by Pdk functions as a metabolic checkpoint for cell cycle quiescence in hematopoietic stem cells. Cell Stem Cell *12*, 49–61.

Tohyama, S., Hattori, F., Sano, M., Hishiki, T., Nagahata, Y., Matsuura, T., Hashimoto, H., Suzuki, T., Yamashita, H., Satoh, Y., et al. (2013). Distinct metabolic flow enables large-scale purification of mouse and human pluripotent stem cell-derived cardiomyocytes. Cell Stem Cell *12*, 127–137.

Umeda, K., Suzuki, K., Yamazoe, T., Shiraki, N., Higuchi, Y., Tokieda, K., Kume, K., Mitani, K., and Kume, S. (2013). Albumin gene targeting in human embryonic stem cells and induced pluripotent stem cells with helper-dependent adenoviral vector to monitor hepatic differentiation. Stem Cell Res. (Amst.) *10*, 179–194.

Wang, J., Alexander, P., Wu, L., Hammer, R., Cleaver, O., and McKnight, S.L. (2009). Dependence of mouse embryonic stem cells on threonine catabolism. Science *325*, 435–439.

Wellen, K.E., and Thompson, C.B. (2012). A two-way street: reciprocal regulation of metabolism and signalling. Nat. Rev. Mol. Cell Biol. *13*, 270–276.

Zhang, X., Neganova, I., Przyborski, S., Yang, C., Cooke, M., Atkinson, S.P., Anyfantis, G., Fenyk, S., Keith, W.N., Hoare, S.F., et al. (2009). A role for NANOG in G1 to S transition in human embryonic stem cells through direct binding of CDK6 and CDC25A. J. Cell Biol. *184*, 67–82.

Cell Metabolism, Volume *19*

Supplemental Information

Methionine Metabolism Regulates Maintenance and Differentiation of Human Pluripotent Stem Cells

Nobuaki Shiraki, Yasuko Shiraki, Tomonori Tsuyama, Fumiaki Obata, Masayuki Miura, Genta Nagae, Hiroyuki Aburatani, Kazuhiko Kume, Fumio Endo, and Shoen Kume

Inventory of Supplemental Information

Supplemental Figures and Tables

Supplemental Experimental Procedures

Supplemental References

Figure S1, related to Figure 1.

Impact of amino acid deprivation on undifferentiated human ES/iPS cells

(A) Bright-field images of khES3 cells after culture for 48 hr in complete media or amino acid-deprived media. (B) Impact of graded concentrations of Met treatment for 48 hr on total khES1 or 253G1 cell numbers. (C) TUNEL staining of khES3 cells cultured in complete, Leu (ΔLeu)-, Lys (ΔLys)- or Met (ΔMet)-deprived medium for 48 hr; note that apoptosis was triggered. (D) ΔLeu or ΔLys triggered an increase in G0/G1 khES3 cells. Values represent the mean ± S.E.M. (n = 3). Significant differences were determined by Student's *t*-test; **p < 0.01. Scale bar = 100 μM.

Figure S1 (related to Figure 1)

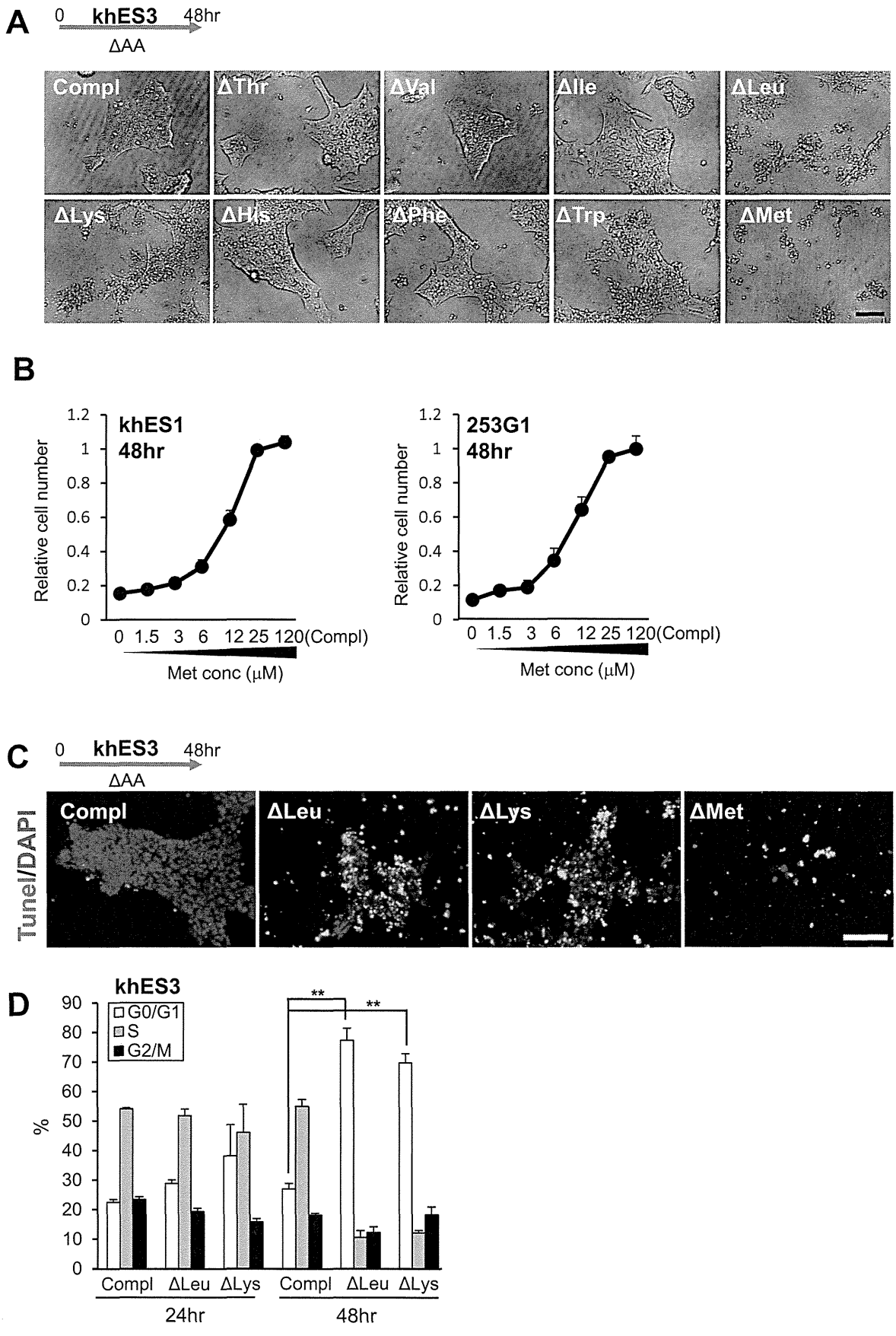

Figure S2, related to Figure 3.

Expression of *MAT2A*, *MAT2B*, and *SMS* are decreased in silenced khES3 cells

Real-time PCR analysis of *MAT2A*, *MAT2B*, or *SMS* in non-silenced (NS) siRNA-treated khES3 cells, *MAT2A*, *MAT2B*, or *SMS* knockdown (KD) khES3 cells. Values represent the mean ± S.E.M. (n = 3). Significant differences were determined by Student's *t*-test; **p < 0.01.

Figure S2 (related to Figure 3)

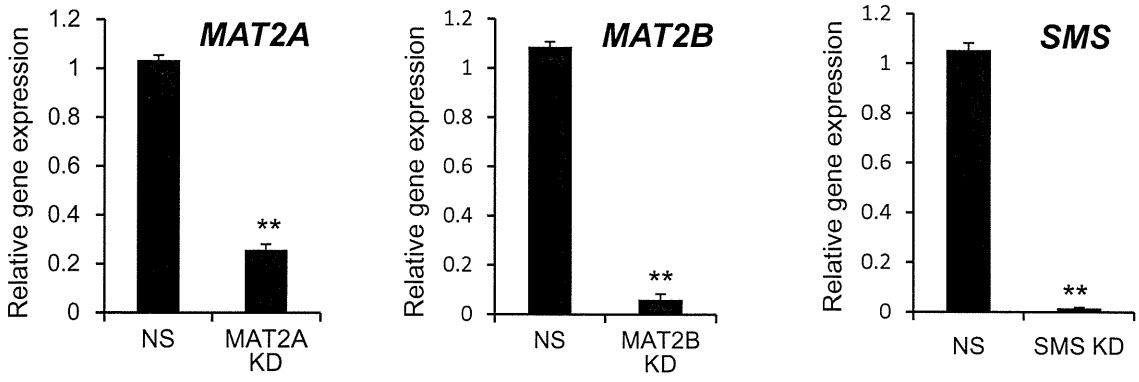

Figure S3, related to Figure 4.

Gene expression analysis of khES3 cells cultured in short-term ΔMet, ΔLeu, or ΔLys conditions

(A) Venn diagram of gene changes greater than 3-fold under Met, Leu, or Lys deprivation for 5 hr compared to those under complete conditions. Genes with signal intensities greater than 50 are shown. (B) Real-time PCR analysis of *DDIT3* (*CHOP*) in khES3 cells cultured in complete or amino acid-deprived media for 5 hr. Values represent the mean ± S.E.M. (n = 3). Significant differences were determined by Student's *t*-test; *$p < 0.05$ and **$p < 0.01$.

Figure S3 (related to Figure 4)

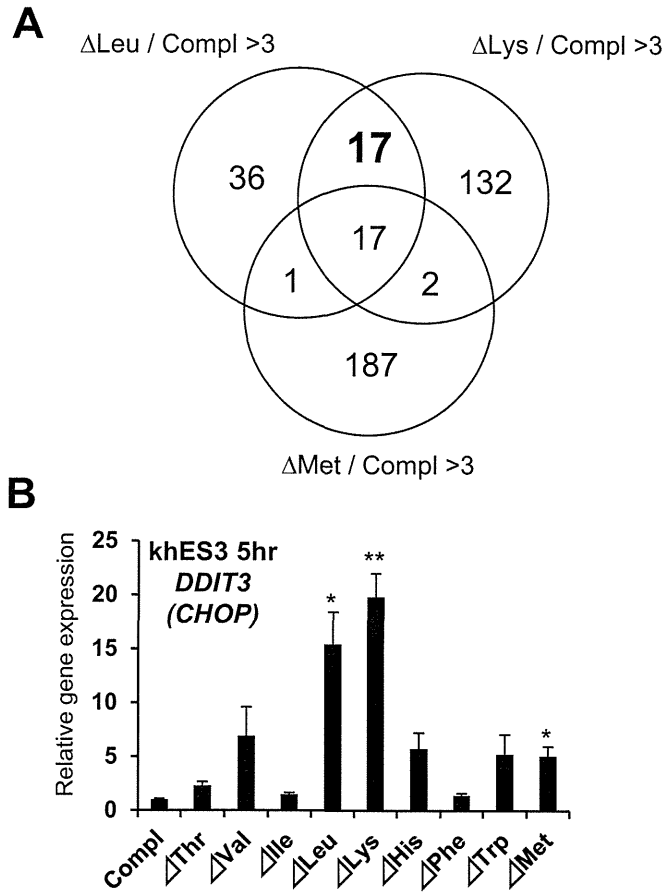

Figure S4, related to Figure 5.

Endoderm differentiation of human ES/iPS cells in Met-deprived media

(A) Met deprivation has little effect on the expression of genes related to endoderm differentiation. Undifferentiated khES3 cells cultured in complete or Met-deprived media for 5 or 24 hr and endoderm cells differentiated for 5 days were used for analysis. (B–D) Human ES/iPS cells pre-cultured in Met-deprived media for 10 hr showed an elevated differentiation into the definitive endoderm. khES1 (B), khES3 (C), or 253G1 cells (D) were used for endoderm differentiation. Values represent the mean ± S.E.M. (n = 3). Significant differences were determined by Student's *t*-test; *$p < 0.05$ and **$p < 0.01$.

Figure S4 (related to Figure 5)